# Assessment of right ventricular strain in children with repaired tetralogy of Fallot using speckle tracking imaging

Jing-Ya Li[1,2], Rong-Juan Li[1], Ning Ma[2], Fang-Yun Wang[2], Xiao-Lin Zhang[2], Jin-Jie Xie[1], Jing Yang[1], Ya Yang[1]

[1]Department of Echocardiography, Beijing Anzhen Hospital, Capital Medical University, Beijing Institute of Heart Lung and Blood Vessel Diseases, Beijing 100029, China; [2]Department of Echocardiography, Beijing Children's Hospital, Capital Medical University, National Center for Children's Health, Beijing 100045, China.

*To the Editor:* Tetralogy of Fallot (TOF) was first surgically repaired in 1955. Initial TOF repairs were performed using a trans-annular right ventricular outflow tract patch to relieve the obstruction. However, this procedure resulted in long-standing pulmonary valve regurgitation and increased right ventricular (RV) volume, causing arrhythmias and sudden death.[1] Thus, pulmonary annulus preservation became the most prevalent surgical strategy for TOF repair, possibly causing a mix of pulmonary stenosis and pulmonary valve regurgitation. Currently, clinicians concerned with RV function decrease during the long-term follow-up use of cardiac magnetic resonance imaging (CMR) to predict the appropriate timing of interventions for valve sparing. Although CMR techniques have evolved as the reference standard for assessing RV volumes and function during the last two decades, routinely monitoring the progression of repaired tetralogy of Fallot (rTOF) RV dysfunction remains difficult. Echocardiographic screening tools can help in estimating RV function and assist clinicians in determining the ideal timing of CMR. Because RV dysfunction is an important clinical outcome indicators,[2] early detection of ventricular function is essential. Echocardiographic evaluation of RV function in rTOF patients is challenging because of the complex ventricle shape. Speckle tracking imaging (STI) provides alternative measurements for quantifying ventricular function. Developments in echocardiography techniques with STI that assess RV functional parameters may provide more sensitive detection, especially when using strain and strain rate (SR). Although STI can evaluate left ventricular function in clinical practice, the value of evaluating RV function in pathologic conditions remains questionable. Here, we evaluated the change of RV deformation parameters during the early phase in pediatric patients after TOF surgery and investigated STI value.

This study included 75 consecutive rTOF subjects who underwent surgery between 2008 and 2016, and derived data were applied between August 2016 and December 2017. Inclusion criteria included patients lacking a change in medical therapy and/or surgical intervention. Exclusion criteria included post-surgical duration of <1 year, arrhythmia, and poor quality of echocardiography resulting in inadequate analysis. Baseline data and surgery information were reviewed for 57 patients. Echocardiographic data of the patients were compared with those of 24 healthy controls. Healthy controls were voluntarily recruited and had neither prior medical or medication history nor current symptoms suggesting cardiovascular disease. They were hospital based and visited the hospital for physical examination. The study was approved by the local research ethics committee. All study participants' parents provided informed consent.

Patients aged <3 years were administered a sedative to reduce restlessness. Two-dimensional (2D) greyscale harmonic images were obtained with patients in the supine position using iE33 or EPIQ 7C ultrasound system (Philips Medical Systems, Bothell, WA, USA) equipped with two transthoracic broadband transducers, S5-1 (1–5 MHz) and S8-3 (3–8 MHz) at a frame rate >70 frames/s. We used the guidelines of the American Society of Echocardiography for RV chamber measurements, RV diameters measured in the apical four chamber view, and measurements of the right ventricular outflow tract were in the parasternal short-axis view. Functional parameters assessments, including fractional area change (FAC), were assessed in the apical four chamber view. FAC was defined as: FAC = (end-diastolic area – end-systolic area)/end-diastolic area. Tricuspid annular plane systolic excursion (TAPSE) was measured as the maximal excursion of the lateral annulus in the apical four-chamber view. All diameter parameters were calculated as applied body surface area (BSA) corrections, and the correction formula was: $BSA = 0.006 \times height + 0.0128 \times weight - 0.153$. We assessed pulmonary stenosis and regurgitation quantitatively by measuring the pressure

Access this article online

Quick Response Code:

Website: www.cmj.org

DOI: 10.1097/CM9.0000000000000126

**Correspondence to:** Dr. Ya Yang, Department of Echocardiography, Beijing Anzhen Hospital, Capital Medical University, Beijing Institute of Heart Lung and Blood Vessel Diseases, Beijing 100029, China
E-Mail: echoyangya99@163.com



Chinese Medical Journal 2019;132(6)

**Received:** 14-01-2019 **Edited by:** Yuan-Yuan Ji

gradient of the pulmonary valve and the width of pulmonary regurgitation orifice in the pulse doppler and color Doppler flow imaging.

Three-dimensional (3D) echocardiography was performed from the apical acoustic window using X5-1 (1–5 MHz) and X7-2 (2–7 MHz) transducers at a frame rate >25 frames/s. RV datasets were acquired separately to include the entire ventricular chamber. Full-volume acquisitioning with the capturing of four adjacent sub-volumes over four consecutive cardiac cycles was performed. Offline analysis was performed using 3D right ventricular analysis software (TomTec Imaging Systems GmBH, Munich, Germany). For quantitative RV analysis, three slices, taken at orthogonal planes (sagittal, short axis, and four chamber view) based on the 3D dataset, were used for automated tracing of the RV endocardium and myocardium border. Single cardiac beats with the best-appearing image quality were used. Both the end-diastolic and end-systolic frames were used for tracking. If tracking proved suboptimal, the border was retraced manually. The right ventricular three-dimensional ejection fraction (3D-EF) was defined as: 3D-EF = (end-diastolic volume – end-systolic volume)/end-diastolic volume. The patients were divided into two groups based on the right ventricular 3D-EF cutoff value in the guidelines for right heart assessment (group I: EF ≥45%; group II: EF <45%).[3]

Automated tracking of myocardial deformation was performed offline using 2D speckle-tracking imaging (TomTec Imaging Systems GmBH, Munich, Germany) for determining the strain and SR. Strain was defined as the percentage change in myocardial deformation, while its derivative, SR, represents the deformation rate of the myocardium over time. Using the standard, apical, four-chamber view, we defined both the endocardium and myocardium of the right ventricle to obtain both the longitudinal and transverse strain and SR. RV was divided into two segments, the free wall and septum. Single cardiac beats with the best-appearing image quality were used, and if tracking was suboptimal, the border was retraced manually. RV parameters assessed included: global longitudinal strain (GLS), free wall longitudinal and transverse strain/strain rate, septum longitudinal and transverse strain/strain rate.

Continuous data are presented as mean ± standard deviation (SD). Categorical data are presented as frequencies. Skew distribution data are presented as median (quartile). To compare normally distributed data between the two groups, we used independent *t* tests. To compare the normally distributed data between multiple groups, we used analysis of variance (ANOVA). Multiple linear regression analyses were performed for the associations between 3D-EF and other characteristics. Intra- and inter-observer agreement of both RV-GLS and 3D-EF were assessed by repeated analysis in one quarter of the datasets, at least half a year after the initial analysis of the same images. The agreement limits between these two measurements were determined as the mean of the differences ± 1.96 SD and presented in a Bland-Altman plot (data not shown). Additionally, the coefficient of variation (the SD of the differences of the two measurements divided by their mean) was calculated. All of the statistical analyses were performed using the Statistical Package for Social Sciences version 21 (SPSS Inc., Chicago, IL, USA). The statistical tests were two sided, and $P < 0.05$ was considered statistically significant.

Thirty-nine patients were male (68%) and 18 were female (32%). The median age at surgery repair was 0.61 (0.49, 0.93) years, mean postoperative duration was 3.8 ± 2.0 years, and mean age at study was 4.7 ± 2.3 years. The patients were divided into two groups based on RV 3D-EF. Group I (3D-EFs ≥45%) included 37 patients, and group II (3D-EFs <45%) included 20 patients. The control group comprised 24 normal children. Baseline characteristics of the study population are shown in the Supplementary Table 1, http://links.lww.com/CM9/A17. Upon comparison of data from three groups and after calculating the body surface area corrections, pulmonary artery parameters in the three groups were equal, but the diameters of the right ventricle were larger in the rTOF groups, and comparison between two rTOF group did not show statistical difference. All RV function parameters were lower in the rTOF group than in the control group, except TAPSE, and group II had much lower parameters than group I. Group II had a more severe stenosis, but the width of regurgitation had no statistical difference. GLS of group II were lower than that of group I; these two groups were lower than in normal children. RV echocardiographic characteristics of rTOF patients and healthy controls are shown in Table 1.

To obtain a 3D-EF predictive model using echocardiographic parameters, we constructed multiple linear regression models. When we excluded both age and postoperative duration that did not influence the model, the best performing model was the one that incorporated both the GLS and FAC data. The equation of the model was: $Y = 15.624 + 0.541 \times \text{FAC} - 0.585 \times \text{GLS}$, $R^2 = 0.570$. The standardized coefficients of FAC and GLS were 0.557 and −0.380, respectively.

We compared all segmental myocardial deformation parameters between the two groups and control group. The longitudinal deformation was determined from the apical four chamber view. The longitudinal SR of free wall, longitudinal strain, and SR of septum, and in group II were lower than healthy controls (free wall SR: −1.29 ± 0.54 *vs.* −0.96 ± 0.26 $s^{-1}$, $P < 0.05$; septum strain: −22.2 ± 3.7% *vs.* −16.7 ± 5.3%, $P < 0.05$; septum SR −1.17 ± 0.43 *vs.* −0.92 ± 0.13 $s^{-1}$, $P < 0.05$), and further lower than group I (free wall SR: −1.24 ± 0.42 *vs.* −0.96 ± 0.26 $s^{-1}$, $P < 0.05$; septum strain: −21.0 ± 4.1% *vs.* −16.7 ± 5.3%, $P < 0.05$; septum SR −1.12 ± 0.36 *vs.* −0.92 ± 0.13 $s^{-1}$, $P < 0.05$).

The transverse deformation of RV free wall and septum were quantified in the apical four-chamber view. Strain analysis revealed that either the free wall or septum had a larger strain in group I compared with the healthy controls (free wall: 30.6 ± 21.9% *vs.* 19.1 ± 17.7%, $P < 0.05$; septum: 37.4 ± 21.5% *vs.* 23.8 ± 13.4%, $P < 0.05$), while group II had no significantly statistical difference compared with the healthy controls. Transverse SR revealed the same characteristics as strain, septum had a larger SR in

**Table 1: RV echocardiographic characteristics of repaired tetralogy of Fallot patients and healthy controls.**

| Characteristics | Controls ($n=24$) | Group I ($n=37$) | Group II ($n=20$) | P |
|---|---|---|---|---|
| Conventional | | | | |
| RV-Base (mm/m$^2$) | 25.1±5.9 | 29.0±4.3* | 27.3±6.2 | 0.029 |
| RV-Middle (mm/m$^2$) | 34.8±6.8 | 44.1±7.4* | 46.6±13.6* | 0.000 |
| RV-Length (mm/m$^2$) | 65.1±10.2 | 78.1±9.0* | 82.8±16.9* | 0.000 |
| RVOT-Prox (mm/m$^2$) | 14.6±3.1 | 21.4±3.4* | 22.9±7.9* | 0.000 |
| RVOT-Distal (mm/m$^2$) | 18.1±3.1 | 22.9±4.1* | 25.1±8.8* | 0.000 |
| PVA (mm/m$^2$) | 20.7±2.8 | 20.9±3.5 | 20.6±3.5 | 0.942 |
| MPA (mm/m$^2$) | 22.1±3.5 | 21.1±3.2 | 20.4±4.7 | 0.325 |
| LPA (mm/m$^2$) | 10.8±2.4 | 11.3±2.6 | 10.0±2.8 | 0.181 |
| RPA (mm/m$^2$) | 10.8±2.3 | 11.2±2.7 | 10.0±1.9 | 0.199 |
| Functional | | | | |
| TAPSE (mm/m$^2$) | 18.5±4.8 | 19.7±5.4 | 17.4±4.8 | 0.272 |
| FAC (%) | 48.9±5.5 | 41.2±7.0* | 32.7±4.6*,† | 0.000 |
| 3D-EF (%) | 59.0±4.4 | 52.1±5.2* | 40.8±3.7*,† | 0.000 |
| GLS (%) | −24.0±3.4 | −21.8±4.2* | −17.3±4.9*,† | 0.000 |
| Color Doppler flow | | | | |
| Pressure gradient of pulmonary valve (mmHg) | 3.8±1.0 | 20.9±10.3* | 26.2±12.9*,† | 0.000 |
| Width of regurgitation (mm) | 0 | 7.2±3.1* | 8.1±2.9* | 0.000 |

All values are presented as mean±standard deviation. *$P<0.05$ compared with controls. †$P<0.05$ compared with group I. 3D-EF: Three-dimensional ejection fraction; FAC: Fractional area change; GLS: Global longitudinal strain; LPA: Left pulmonary artery; MPA: Main pulmonary artery; PVA: Pulmonary valve annulus; RPA: Right pulmonary artery; RV: Right ventricle; RVOT: Right ventricular outflow tract; TAPSE: Tricuspid annular plane systolic excursion.

group I compared with the healthy controls (2.00±0.81 *vs.* 1.12±0.61 s$^{-1}$, $P<0.05$). Meanwhile, the septum transverse strain and SR were lower in group II compared with group I (strain: 37.4±21.5% *vs.* 26.1±15.7%, $P<0.05$; SR: 2.00±0.81 vs. 1.45±0.63 s$^{-1}$, $P<0.05$). The results are shown in Figure 1.

We performed intra-observer and inter-observer agreement analyses. The coefficients of variation for the intra-observer measurements were 8.0% for 3D-EF and 10.9% for GLS. The coefficients of variation for the inter-observer measurements were 8.7% for 3D-EF and 14.3% for GLS. Bland-Altman plots demonstrating intra-observer and inter-observer agreement are shown in the Supplementary Figure 1, http://links.lww.com/CM9/A17.

In this study, RV function, including 3D-EF and GLS, was decreased slightly in rTOF patients. The transverse strain and SR were increased significantly in patients with normal EF, which indicated a potential preservation of RV myocardial function.

The mean time of post-surgical duration for the study population was 3.8±2.0 years. The diameter parameters of rTOF patients were larger than those of the healthy controls, which indicated RV enlargement. Although nine patients had NYHA classification grade II, we found that all parameters of RV function, including TAPSE, FAC, and 3D-EF, were within normal range in group I and slightly decreased in group II. However, except TAPSE, the other parameters of RV function were worse in rTOF patients than in healthy controls. During that time, we observed that the level of pulmonary valve stenosis was mild to moderate in our patients and the width of regurgitation in two rTOF groups were not statistically different. Unlike previous studies for adult patients,[4] we found a few patients with RV dysfunction by echocardiography during the early phase. Most rTOF patients had preserved RV function in the short phase.

We used the STI to analyze the global longitudinal deformation function of RV. Compared with the healthy controls, right ventricular GLS was decreased in the rTOF patient population. The mean value in group II was lower than that in group I, implying a lower GLS coordinated with a worse EF. In normal RV anatomy, longitudinal contraction is the major contributor to the overall RV performance.[5] Under resting and loaded conditions, GLS was a reliable parameter that reflected RV function.[6] Decreased RV longitudinal strain in rTOF patients may be a marker of early RV dysfunction and correlates with CMR-derived EF.[7] We used multiple linear regression analysis to further understand the relationships between 3D-EF and systolic function parameters. FAC and GLS were correlated with 3D-EF; FAC had a greater effect on the 3D-EF according to the larger standardized coefficient. Our results are supported by previous studies.[8] Although GLS is an index of RV function, the single parameter does not fully represent the RV function. Thus, other useful deformation parameters should be assessed.

RV segmental strain and SR offline analysis was based on the RV algorithms, which were not a simple application of the left ventricular algorithms. The modeling divided RV into two segments: the free wall and septum. In the longitudinal axis of the septum strain and SR, free wall SR was lower than patients with impaired RV systolic function. While we performed in the transverse axis, RV transverse strain and SR in patients with normal 3D-EF increased, which was reported previously.[9] In the study, the radial strain and SR on the right side of the septum was significantly increased in TOF patients compared with

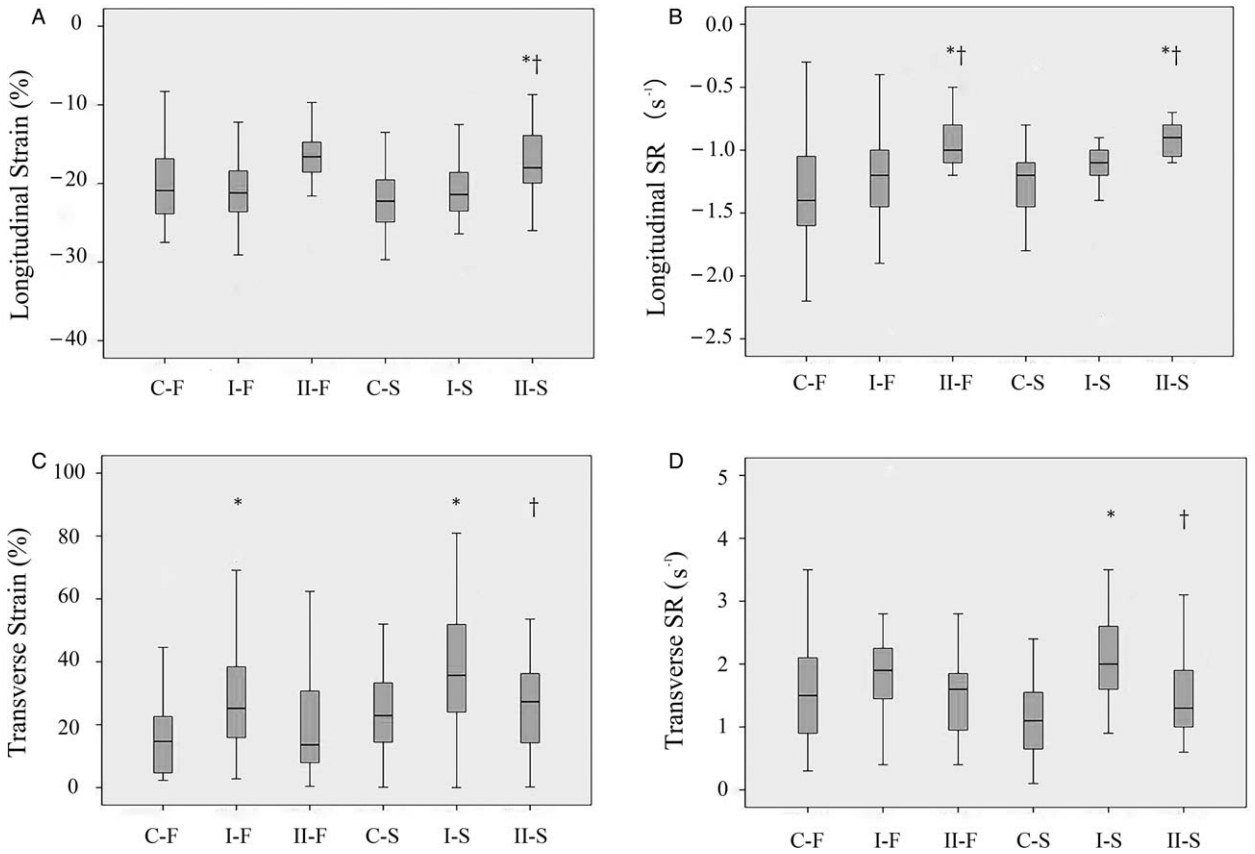


**Figure 1:** (A) Longitudinal strain of the rTOF patient and healthy controls. (B) Longitudinal SR of the rTOF patient and healthy controls. (C) Transverse strain of the rTOF patient and healthy controls. (D) Transverse SR of the rTOF patient and healthy controls. Boxes describe the distribution of peak longitudinal strain/SR (25th and 75th percentiles; the central line represents the median). Vertical lines represent the range between the 5th and 95th percentiles; $^{*}P<0.05$, *vs.* healthy controls, $^{\dagger}P<0.05$, *vs.* group I. C represents controls; I represents group I; II represents group II; F represents the free wall; S represents septum. SR: Strain rate; rTOF: Repaired tetralogy of Fallot.

healthy controls and atrial septal defect patients. The phenomenon occurred in the circumferential strain in another study of rTOF patients and in the radial strain as well.[10] 2D and 3D values of circumferential strain were higher in patients after rTOF than in healthy controls. In our study, we determined that the increase in transverse strain and SR of RV occurred in patients with a normal RV 3D-EF, suggesting a pre-clinical compensative change before 3D-EF and longitudinal strain decrease. The mechanism of this increased strain parameter remains unclear. The mechanism of deformation compensation in the short axis might be related to the right ventricular myocardial hypertrophy and needs further exploration.

We found higher variability in GLS measurements than in 3D-EFs, possibly explaining that the RV free wall was difficult to image. The RV-GLS analysis comprised only two segments; therefore, the image quality of the free wall was significant. However, 3D echocardiography involved the comprehensive tracking of the RV membrane; therefore, the influence of the RV free wall image quality was less pronounced. Even with the higher variability in GLS measurements, there was good reproducibility according to the coefficients of variation. Intra- and inter-observer variation of GLS and 3D-EF measurements were considerable.

In our study of the short-term post-surgical duration of rTOF patients, either dysfunction or preservation of RV function was revealed by STI, which were efficient diagnostic technique for detecting RV function. Compared with GLS, segmental parameters, including transverse strain and SR, might be valuable parameters for suggesting pre-clinical changes in RV function. If we could continue to observe these parameters, which changed during the short-term period, we could relate these parameters to patient outcomes. Moreover, STI could be used regularly for clinical monitoring, which is the main advantage of this technique.

## Declaration of patient consent

The authors certify that they have obtained all appropriate patient consent forms. In the form the patients have given their consent for their images and other clinical information to be reported in the journal. The patients understand that their names and initials will not be published and due efforts will be made to conceal their identity, but anonymity cannot be guaranteed.

## Conflict of interest

None.

## References


1. Gatzoulis MA, Balaji S, Webber SA, Siu SC, Hokanson JS, Poile C, *et al*. Risk factors for arrhythmia and sudden cardiac death late after repair of tetralogy of Fallot: a multicentre study. Lancet 2000;356:975–981. doi: 10.1016/S0140-6736(00)02714-8.
2. Knauth AL, Gauvreau K, Powell AJ, Landzberg MJ, Walsh EP, Lock JE, *et al*. Ventricular size and function assessed by cardiac MRI predict major adverse clinical outcomes late after tetralogy of Fallot repair. Heart 2008;94:211–216. doi: 10.1136/hrt.2006.104745.
3. Rudski LG, Lai WW, Afilalo J, Hua L, Handschumacher MD, Chandrasekaran K, *et al*. Guidelines for the echocardiographic assessment of the right heart in adults: a report from the American Society of Echocardiography endorsed by the European Association of Echocardiography, a registered branch of the European Society of Cardiology, and the Canadian Society of Echocardiography. J Am Soc Echocardiogr 2010;23:685–713. doi: 10.1016/j.echo.2010.05.010.
4. Sabate RA, Bonnichsen CR, Reece CL, Connolly HM, Burkhart HM, Dearani JA, *et al*. Long-term follow-up in repaired tetralogy of fallot: can deformation imaging help identify optimal timing of pulmonary valve replacement? J Am Soc Echocardiogr 2014;27:1305–1310. doi: 10.1016/j.echo.2014.09.012.
5. Haddad F, Hunt SA, Rosenthal DN, Murphy DJ. Right ventricular function in cardiovascular disease, part I: Anatomy, physiology, aging, and functional assessment of the right ventricle. Circulation 2008;117:1436–1448. doi: 10.1161/CIRCULATIONAHA.107.653576.
6. Toro KD, Soriano BD, Buddhe S. Right ventricular global longitudinal strain in repaired tetralogy of Fallot. Echocardiography 2016;33:1557–1562. doi: 10.1111/echo.13302.
7. Li Y, Xie M, Wang X, Lu Q, Zhang L, Ren P. Impaired right and left ventricular function in asymptomatic children with repaired tetralogy of Fallot by two-dimensional speckle tracking echocardiography study. Echocardiography 2015;32:135–143. doi: 10.1111/echo.12581.
8. Bonnemains L, Stos B, Vaugrenard T, Marie PY, Odille F, Boudjemline Y. Echocardiographic right ventricle longitudinal contraction indices cannot predict ejection fraction in post-operative Fallot children. Eur Heart J Cardiovasc Imaging 2012;13:235–242. doi: 10.1093/ejechocard/jer263.
9. Hayabuchi Y, Sakata M, Ohnishi T, Kagami S. A novel bilayer approach to ventricular septal deformation analysis by speckle tracking imaging in children with right ventricular overload. J Am Soc Echocardiogr 2011;24:1205–1212. doi: 10.1016/j.echo.2011.06.016.
10. Berganza FM, de Alba CG, Özcelik N, Adebo D. Cardiac magnetic resonance feature tracking biventricular two-dimensional and three-dimensional strains to evaluate ventricular function in children after repaired tetralogy of Fallot as compared with healthy children. Pediatr Cardiol 2017;38:566–574. doi: 10.1007/s00246-016-1549-6.


**How to cite this article:** Li JY, Li RJ, Ma N, Wang FY, Zhang XL, Xie JJ, Yang J, Yang Y. Postoperative acute kidney failure and incision skin necrosis caused by a giant retroperitoneal paraganglioma. Chin Med J 2019;132:744–748. doi: 10.1097/CM9.0000000000000126